

Molecular characterization of NbEH1 and NbEH2, two epoxide hydrolases from *Nicotiana benthamiana*

Fong-Chin Huang, Wilfried Schwab*

Technische Universität München, Biotechnology of Natural Products, Liesel-Beckmann-Str. 1, Freising D-85354, Germany

ARTICLE INFO

Article history:

Received 29 January 2013

Accepted 28 February 2013

Available online 3 April 2013

Keywords:

Epoxide hydrolase

Peroxygenase

Nicotiana benthamiana

Epoxide

Diol

Triol

ABSTRACT

Plant epoxide hydrolases (EH) form two major clades, named EH1 and EH2. To gain a better understanding of the biochemical roles of the two classes, *NbEH1.1* and *NbEH2.1* were isolated from *Nicotiana benthamiana* and *StEH* from potato and heterologously expressed in *Escherichia coli*. The purified recombinant proteins were assayed with a variety of substrates. *NbEH1.1* only accepted some aromatic epoxides, and displayed the highest enzyme activity towards phenyl glycidyl ether. In contrast, *NbEH2.1* displayed a broad substrate range and similar substrate specificity as *StEH*. The latter enzymes showed activity towards all fatty acid epoxides examined. The activity (V_{max}) of *NbEH1.1* towards phenyl glycidyl ether was 10 times higher than that of *NbEH2.1*. On the contrary, *NbEH2.1* converted *cis*-9,10-epoxystearic acid with V_{max} of 3.83 $\mu\text{mol min mg}^{-1}$ but *NbEH1.1* could not hydrolyze *cis*-9,10-epoxystearic acid. Expression analysis revealed that *NbEH1.1* is induced by infection with tobacco mosaic virus (TMV) and wounding, whereas *NbEH2.1* is present at a relatively constant level, not influenced by treatment with TMV and wounding. *NbEH1.1* transcripts were present predominantly in roots, whereas *NbEH2.1* mRNAs were detected primarily in leaves and stems. Overall, these two types of tobacco EH enzymes are distinguished not only by their gene expression, but also by different substrate specificities. EH1 seems not to participate in cutin biosynthesis and it may play a role in generating signals for activation of certain defence and stress responses in tobacco. However, members of the EH2 group hydrate fatty acid epoxides and may be involved in cutin monomer production in plants.

© 2013 Elsevier Ltd. All rights reserved.

1. Introduction

Epoxide hydrolases (EH, EC 3.3.2.3) catalyze the conversion of epoxides to their corresponding vicinal diols. These enzymes are found in various species of mammals, insects, fungi, bacteria and plants. The functions of mammalian EHs are diverse, including regulation of inflammation, xenobiotic detoxification and drug metabolism (Newman et al., 2005; Morisseau and Hammock, 2005). For microorganisms, EHs seem important in the catabolism of specific carbon sources from natural sources, such as limonene (Van der Werf et al., 1999). Plant EHs appear to play a role in the biosynthesis of monomers of cutin, a polymer that accumulates in cell walls of damaged tissues (Blée and Schuber, 1993; Blée, 1998). Cutin is important in plant development, protection from environmental stresses, and disease resistance (Kato et al., 1983; Kiyosue et al., 1994; Pinot et al., 2000). In addition to its participation in cutin biosynthesis, EH may have other roles during plant defence responses. Expression of a cytosolic EH of *Citrus jambhiri* increased upon inoculation with the pathogen *Alternaria alternata*, but transcripts were not detected in healthy leaves (Gomi et al., 2003).

* Corresponding author. Tel.: +49 8161 712912; fax: +49 8161 712950.
E-mail address: schwab@wzw.tum.de (W. Schwab).

NtEH1, a cytosolic EH from *Nicotiana tabacum*, was induced during the hypersensitive response to tobacco mosaic virus but was not affected in the compatible interaction (Guo et al., 1998). Resistant plants often exhibit a rapid and localized cell death at the site of pathogen infection, termed the hypersensitive response. This rapid cell death process is thought to help prevent pathogen multiplication and spread. *NbEH1.1* in *Nicotiana benthamiana* showed increased expression during compatible interactions with the hemibiotrophic fungal pathogens, *Colletotrichum destructivum* and *Colletotrichum orbiculare*, and the hemibiotrophic bacterial pathogen, *Pseudomonas syringae* pv. *tabaci* (Wijekoon et al., 2008). In addition, epoxides are usually reactive causing toxicity to cells. Hence, another role for EHs in plants would be to break down epoxides accumulating during stress into less reactive compounds (Murray et al., 1993).

In plants, EHs have been characterized from several organisms, such as broad bean (Hamberg and Fahlstadius, 1992), soybean (Blée and Schuber, 1992a,b; Blée and Schuber, 1995; Arahira et al., 2000; Blée et al., 2005), *Arabidopsis* (Kiyosue et al., 1994), potato (Stapleton et al., 1994; Morisseau et al., 2000; Elfström and Widersten, 2005; Mowbray et al., 2006), tobacco (Guo et al., 1998), *Brassica napus* (Bellevik et al., 2002), and *Euphorbia lagascae* (Edqvist and Farbos, 2003). The epoxide hydrolase from potato

(StEH1) is the best characterized plant EH. The expression of StEH1 was found to be regulated by both developmental and environmental signals. Its mRNA was observed to accumulate on wounding and application of exogenous methyl jasmonate (Stapleton et al., 1994). The polypeptide encoded by StEH1 is similar to mammalian soluble EH both in sequence and enzymatic properties. The recombinant StEH1 enzyme hydrolyzed a commonly used diagnostic substrate for the soluble form of mammalian EH. Inhibitor profiles of the recombinant StEH1 and mammalian soluble EH were also similar (Stapleton et al., 1994; Morisseau et al., 2000). Another well characterized plant EH is soybean fatty acid EH (Blée and Schuber, 1992a,b, Blée and Schuber, 1995; Blée et al., 2005). It is quite specific for fatty epoxides. This enzyme hydrates preferentially 9(R),10(S)-epoxy-12(Z)-octadecenoic and 12(R),13(S)-epoxy-9(Z)-octadecenoic acid (Blée and Schuber, 1992a).

Comparison of the protein sequences of EHs from plants revealed two major clades, which are named EH1 and EH2 (Wijekoon et al., 2008). Both EH1 and EH2 type sequences have been found in many plants, such as *Allium cepa*, *Hordeum vulgare*, *Nicotiana benthamiana*, *Nicotiana tabacum*, *Capsicum annuum*, *Solanum tuberosum*, *Oryza sativa* and *Triticum aestivum*. However, an exception was the *Arabidopsis thaliana* genome, which contains 33 EH genes that are all of the EH2 type (Wijekoon et al., 2008). Four EHs have been found in *N. benthamiana*, namely NbEH1.1 and NbEH1.2 of the EH1 clade and NbEH2.1 and NbEH2.2 of the EH2 clade (Wijekoon et al., 2008, 2011). Motif analysis among 30 EH1 and EH2 from Solanaceae plants showed differences primarily in the lid region around the catalytic site. *In silico* models of 3D structures also showed significant differences in the lid region between NbEH1.1 and NbEH2.1 (Wijekoon et al., 2011). NbEH2.1 and NbEH2.2 have a predicted peroxisomal targeting sequence, catalytic triad, and structural similarities to a potato epoxide hydrolase (StEH1) (Mowbray et al., 2006; Thomaus et al., 2008). Besides, the gene expression levels of NbEH1.1, NbEH1.2, NbEH2.1, and NbEH2.2 in response to different pathogens have been analyzed (Wijekoon et al., 2008, 2011). The results showed that the expression pattern of NbEH1 was different from that of NbEH2, demonstrating specialization among EH genes in basal resistance.

To gain a better understanding of the molecular mechanism and the biochemical roles of EH1 and EH2 in plants, and to explore potential biotechnological applications, NbEH1.1 and NbEH2.1 were isolated from *N. benthamiana* as well as StEH from potato and heterologously expressed in *Escherichia coli*. The purified recombinant proteins were assayed for their enzymatic activities with a variety of epoxide substrates and the formation of fatty acid diols was ana-

lyzed in detail. In addition, the expression patterns of these two EH isoforms were examined to disclose their potential biological functions.

2. Results and discussion

2.1. Heterologous expression and purification of NbEH1.1, NbEH2.1 and StEH

Full-length cDNAs of NbEH1.1 and NbEH2.1 genes were isolated from leaf of *N. benthamiana*, whereas that of StEH gene was isolated from potato tuber. The open reading frames of NbEH1.1, NbEH2.1 and StEH were cloned into the pQE30 vector for expression in *E. coli* to characterize the catalytic activities of the encoded proteins. The protein sequence length of NbEH1.1, NbEH2.1 and StEH is 311, 315 and 321 amino acids, respectively. NbEH1.1 is 35% and 34% identical to NbEH2.1 and StEH, respectively, while NbEH2.1 is 61% identical to StEH. Furthermore, the recombinant proteins were purified using His-tag purification system. The proteins were separated on a 10% SDS–polyacrylamide gel and visualized by Coomassie staining. The stained gel showed the recombinant NbEH1.1, NbEH2.1, and StEH proteins with molecular size of ca. 37.6 kDa, 37.7 kDa, and 38.4 kDa, respectively (Fig. 1A–C). A large amount of NbEH1.1 protein was expressed and purified to homogeneity. Although NbEH2.1 protein was less expressed, it could be purified to homogeneity. However, many other proteins were still detected in the purified fractions of StEH. An another vector pET29a(+) was also used to express NbEH2.1 and StEH proteins, however, less amount and lower purity of proteins were obtained (data not shown).

2.2. Functional analysis of NbEH1.1, NbEH2.1 and StEH proteins

Purified EH proteins were used for enzyme activity assays towards a variety of substrates. Product formation was confirmed by LC–MS and GC–MS. The used substrates can be grouped into four classes: aromatic epoxides, terminal aliphatic epoxides, limonene oxides and fatty acid epoxides (Supplementary Fig. S1A–D). All substrates were also incubated with negative (empty vector) controls. No diol products were formed in the control experiments. NbEH1.1 only showed activity with artificial substrates such as phenyl glycidyl ether and styrene oxide (Table 1). Phenyl glycidyl ether was the preferred substrate and the activity of NbEH1.1 towards this aromatic epoxide was even higher than that of NbEH2.1.

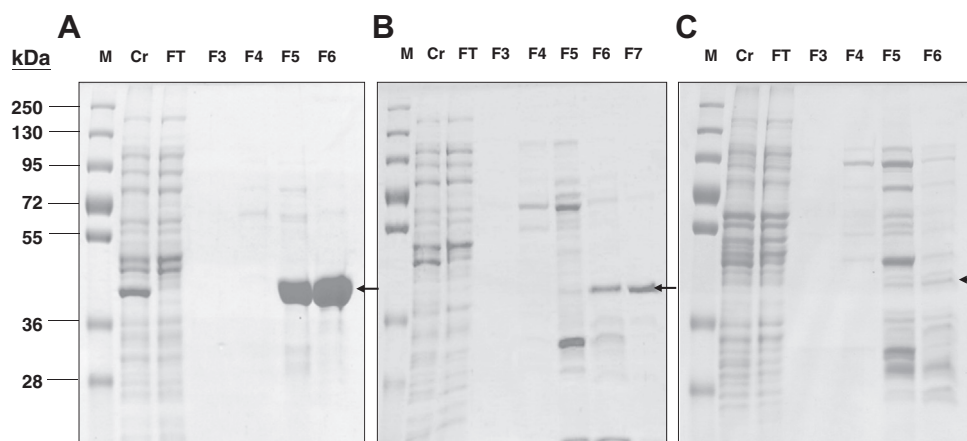


Fig. 1. Coomassie-stained polyacrylamide gel analysis of recombinant EH proteins expressed in the pQE30 vector system. (A) Purification of NbEH1.1 protein: purified protein fractions (F3–F6). (B) Purification of NbEH2.1 protein: purified protein fractions (F3–F7). (C) Purification of StEH protein: purified protein fractions (F3–F6). M: Marker; Cr: total protein; FT: flow through. The purified proteins were indicated by arrows (→).

Table 1
The catalytic activities of recombinant NbeH1.1, NbeH2.1, and StEH towards various epoxide substrates. Activities were determined by LC–MS and GC–MS. Values are the means of two or three separate determinations. Measurements were performed with purified protein. Epoxide structures are shown in Supplementary Fig. S1. The lower detection limit of reaction progress is 0.001 $\mu\text{mol min}^{-1} \text{mg}^{-1}$.

Substrates	NbeH1 ($\mu\text{mol min}^{-1} \text{mg}^{-1}$)	NbeH2 ($\mu\text{mol min}^{-1} \text{mg}^{-1}$)	StEH ($\mu\text{mol min}^{-1} \text{mg}^{-1}$)
<i>cis</i> -Stilbene oxide	–	–	0.003 \pm 0.0002
<i>trans</i> -Stilbene oxide	–	0.068 \pm 0.004	0.244 \pm 0.016
<i>trans</i> -1,3-Diphenyl-2,3-epoxypropan-1-one	–	0.043 \pm 0.002	0.009 \pm 0.0002
Phenyl glycidyl ether	0.268 \pm 0.019	0.022 \pm 0.001	0.235 \pm 0.003
Styrene oxide	0.114 \pm 0.005	0.030 \pm 0.0002	0.749 \pm 0.049
1,2-Epoxy-pentane	–	–	–
Glycidyl isopropyl ether	–	–	–
<i>cis</i> - α -Limonene-1,2-oxide	–	–	–
<i>cis</i> - β -Limonene-1,2-oxide	–	–	–
<i>trans</i> - α -Limonene-1,2-oxide	–	–	–
<i>trans</i> - β -Limonene-1,2-oxide	–	–	–
<i>cis</i> -9,10-Epoxy-stearic acid	–	1.142 \pm 0.017	1.145 \pm 0.092
<i>cis</i> -9,10-Epoxy-12-octadecenoic acid	–	0.552 \pm 0.217	1.305 \pm 0.216
<i>cis</i> -12,13-Epoxy-9-octadecenoic acid	–	0.699 \pm 0.275	1.504 \pm 0.249
12,13-Epoxy-9-HOD	–	0.026 \pm 0.003	0.244 \pm 0.048
<i>cis</i> -11,12-Epoxy-eicosanoic acid	–	0.532 \pm 0.072	0.560 \pm 0.108

Table 2
Comparison of kinetic properties for recombinant NbeH1.1 and NbeH2.1 measured using phenyl glycidyl ether and *rac cis*-9,10-epoxystearic acid as substrates. Values are the means of three separate determinations. One unit of activity (U) corresponds to the amount of enzyme that converts 1 μmol of substrate per minute.

	NbeH1.1	NbeH2.1
Substrate phenyl glycidyl ether		
Temperature optimum	50 °C	40 °C
pH optimum	10	7
K_m (mM)	2.30 \pm 0.28	0.51 \pm 0.05
V_{max} (U mg^{-1})	1.30 \pm 0.04	0.13 \pm 0.01
V_{max}/K_m (U $\text{mg}^{-1} \text{mM}^{-1}$)	0.58 \pm 0.06	0.26 \pm 0.02
Substrate <i>rac cis</i> -9,10-epoxystearic acid	No activity	
Temperature optimum	–	40 °C
pH optimum	–	pH 8
K_m (mM)	–	0.17 \pm 0.02
V_{max} (U mg^{-1})	–	3.83 \pm 0.40
V_{max}/K_m (U $\text{mg}^{-1} \text{mM}^{-1}$)	–	23.38 \pm 2.29

Fatty acid epoxides were not hydrolyzed by NbeH1.1 and no diol products were detected even after 20 h incubation. In contrast, the EH2 clade members NbeH2.1 and StEH showed similar enzyme activities towards all substrates examined and a broad substrate range. In contrast to NbeH1.1, NbeH2.1 and StEH showed high enzyme activity towards fatty acid epoxides. 1,2-Epoxy-pentane, glycidyl isopropyl ether, and any limonene epoxides were not converted by the three enzymes. NbeH1.1 and NbeH2.1 showed clear differential substrate specificity. This may indicate that they play diverse biochemical roles in plants.

In order to gain more details about the catalytic properties of NbeH1.1 and NbeH2.1, the kinetic characteristics of phenyl glycidyl ether and *cis*-9,10-epoxystearic acid were determined for these two enzymes (Table 2). The enzymatic activities of NbeH1.1 and NbeH2.1 were analyzed at different pH values (pH 2–12) and temperatures (15–60 °C) to find out the optimal catalytic conditions (Supplementary Fig. S2). The recombinant NbeH1.1 enzyme has a temperature and pH optimum at 50 °C and pH 10, respectively with phenyl glycidyl ether as substrate. The K_m for this substrate was 2.3 mM (Table 2). For the same substrate NbeH2.1 has a temperature optimum at 40 °C and a pH optimum of pH 7. The K_m for this substrate was 0.51 mM. In addition, the recombinant NbeH2.1 enzyme has a temperature optimum at 40 °C and a pH optimum of pH 8 with *cis*-9,10-epoxystearic acid as a substrate. The K_m for this substrate was 0.17 mM (Supplementary Fig. S3). However, no product was formed from *cis*-9,10-epoxystearic acid by NbeH1.1, even after 20 h incubation. Taken together, the

NbeH1.1 protein preferred alkaline (pH 10) and NbeH2.1 neutral pH values (pH 7–8). Both enzymes preferred relative high temperature. A EH enzyme cloned from *Brassica napus* (Bellevik et al., 2002) whose amino acid sequence is 57% identical to NbeH2.1 also preferred high temperature (55 °C) and preferred neutral pH values (pH 6–7) like NbeH2.1. The activity (V_{max}) of NbeH1.1 towards phenyl glycidyl ether was 10 times higher than that of NbeH2.1. On the contrary, NbeH2.1 converted *cis*-9,10-epoxystearic acid efficiently but NbeH1.1 could not hydrolyze *cis*-9,10-epoxystearic acid.

2.3. Metabolism of fatty acids by PXG and EH

The peroxygenase (PXG) cascade constitutes an additional branch to the lipoxygenase pathway (Blée and Schubert, 1993; Blée, 1998). PXG catalyzes, in higher plants, the efficient hydroperoxide-dependent epoxidation of unsaturated fatty acids such as oleic and linoleic acid (Blée and Schubert, 1990; Hamberg and Hamberg, 1990; Hamberg and Fahlstadius, 1992; Blée, 1998). In addition to PXG, this cascade also involves EH that catalyzes the *trans*-hydration of fatty acid *cis*-epoxides into their corresponding dihydrodiols. To gain more knowledge about the metabolism pathway of fatty acids catalyzed by PXG and EH, various fatty acids and fatty acid hydroperoxide were added to reaction mixtures that contained PXG and EH. A full-length PXG cDNA, named SIPXG was recently cloned from tomato and expressed in yeast (Aghofack-Nguemezi et al., 2011).

At first, fatty acids were incubated with SIPXG yeast extract at 30 °C in the presence of hydrogen peroxide for 30 min, then purified EH was added and incubated for an additional 30 min. Hydrogen peroxide served as an effective oxygen donor in the peroxygenase reaction. However, for fatty acid hydroperoxide substrates no additional hydroperoxide was required to be added to the reaction. Oleic acid, *cis*-11-eicosenoic acid, linoleic acid, and 9(*S*)-hydroperoxy-10(*E*),12(*Z*)-octadecadienoic acid (9(*S*)-HPOD) were used as substrates. SIPXG converted oleic acid and *cis*-11-eicosenoic acid into *cis*-9,10-epoxystearic acid and *cis*-11,12-epoxy-eicosanoic acid, respectively. The formation of epoxides by SIPXG from linoleic acid, and 9(*S*)-HPOD is described below. Moreover, all fatty acid epoxides formed by SIPXG could be further converted into corresponding diols by NbeH2.1 and StEH. However, no fatty acid epoxides examined could be hydrolyzed into diols by NbeH1.1. The yeast cells containing empty vector (negative control) were also incubated with all fatty acid epoxides examined. No corresponding diol products were detected in the control experiments.

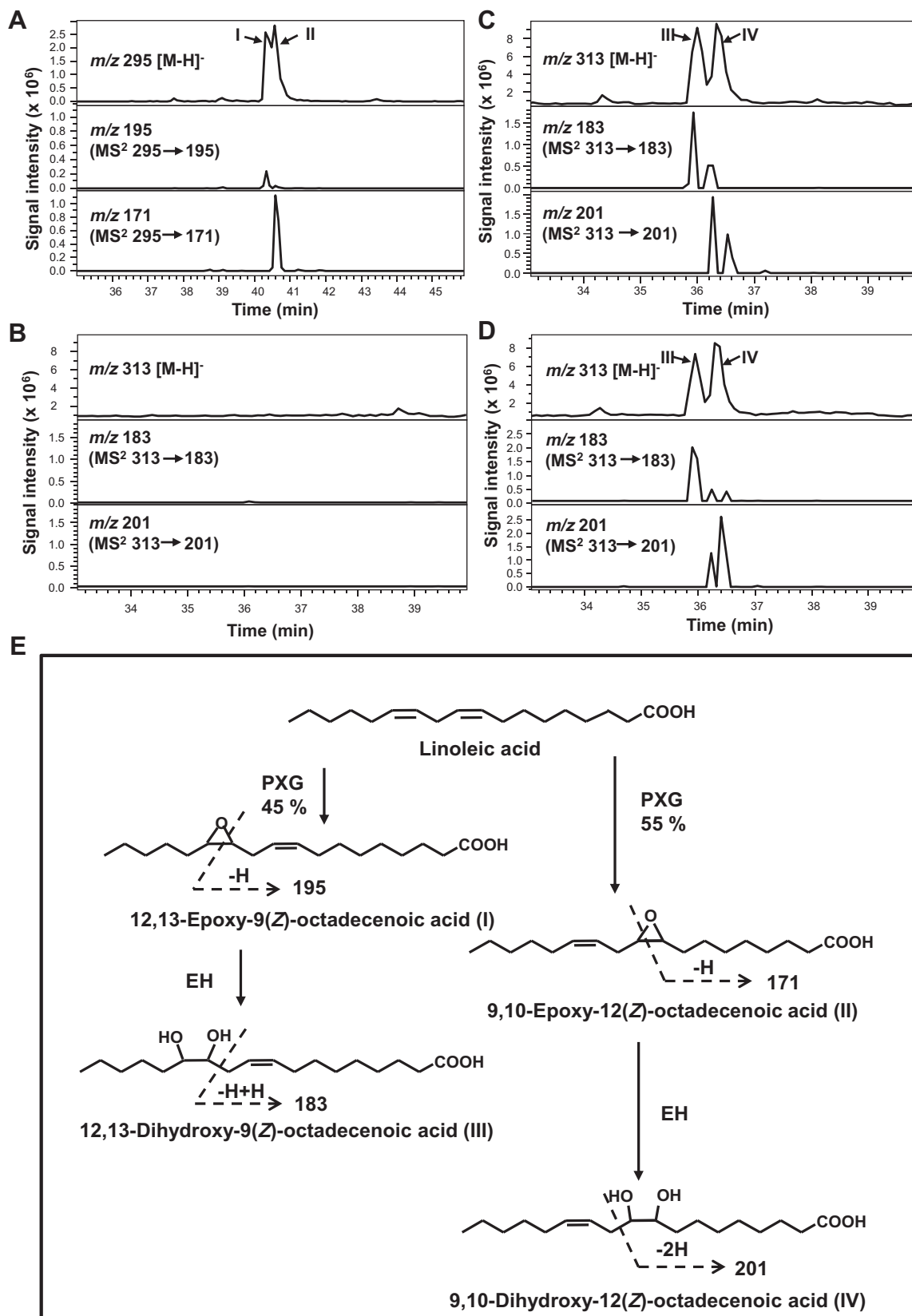


Fig. 2. LC-MS analysis of products formed by incubation of linoleic acid with (A) SIPXG, (B) SIPXG and NbeH1.1, (C) SIPXG and NbeH2.1, and (D) SIPXG and StEH. (E) Metabolism of linoleic acid by PXG and EH. The PXG products 12,13-epoxy-9(Z)-octadecenoate (I) and 9,10-epoxy-12(Z)-octadecenoate (II) were monitored at m/z of 195 and 171, respectively (A). For detection of EH products 12,13-dihydroxy-9(Z)-octadecenoic acid (III) and 9,10-dihydroxy-12(Z)-octadecenoic acid (IV), m/z of 183 and 201 were looked at, respectively (B, C, D). PXG: peroxygenase; EH: epoxide hydrolase.

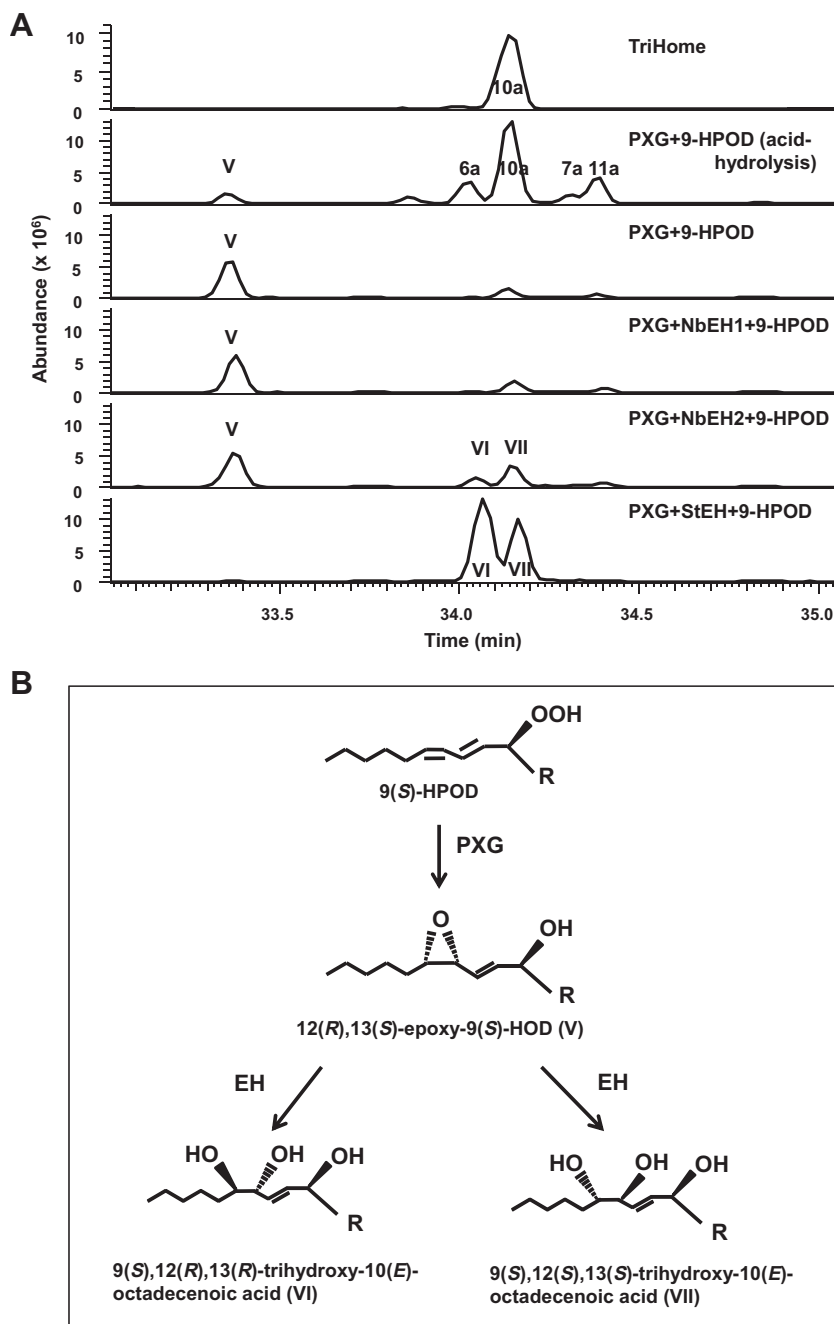


Fig. 3. GC-MS analysis of products generated by incubation of 9(*S*)-HPOD with SIPXG and various EHs. (A) Products were isolated by extraction with ethyl acetate, methylated and trimethylsilylated, then were subjected to GC-MS. TriHome: the reference compound 9(*S*),12(*S*),13(*S*)-trihydroxy-10(*E*)-octadecenoic acid; PXG + 9-HPOD (acid-hydrolysis): 9(*S*)-HPOD was incubated with SIPXG at 30 °C for 30 min, then the reaction solution was acidified to pH 3 and kept at 23 °C for 5 min. Numbers 6a, 7a, 10a and 11a referring to trihydroxyoctadecenoic acid isomers correspond to that previously reported (Hamberg, 1991a; Hamberg and Hamberg, 1996). Peak V (this work) was identified as 12(*R*),13(*S*)-epoxy-9(*S*)-hydroxy-10(*E*)-octadecenoic acid (according to Hamberg and Hamberg, 1996). Peaks VI and VII were identified as 9(*S*),12(*R*),13(*R*)-trihydroxy-10(*E*)-octadecenoic acid (9b) and 9(*S*),12(*S*),13(*S*)-trihydroxy-10(*E*)-octadecenoic acid (10a), respectively (according to Hamberg, 1991a). (B) Metabolism of 9(*S*)-HPOD by PXG and EH. R: (CH₂)₇-COOH; 9(*S*)-HPOD: 9(*S*)-hydroperoxy-10(*E*),12(*Z*)-octadecadienoic acid; 12(*R*),13(*S*)-epoxy-9(*S*)-HOD: 12(*R*),13(*S*)-epoxy-9(*S*)-hydroxy-10(*E*)-octadecenoic acid; PXG: peroxygenase; EH: epoxide hydrolase.

The oxidation of linoleic acid by SIPXG yielded two positional monoepoxide isomers, namely *cis*-12,13-epoxy-9(*Z*)-octadecenoate (I) and *cis*-9,10-epoxy-12(*Z*)-octadecenoate (II) (Fig. 2A and E) and corresponds to that of a previous study (Blée and Schuber, 1990). *cis*-12,13-Epoxy-9(*Z*)-octadecenoate and *cis*-9,10-epoxy-12(*Z*)-octadecenoate were further converted into 12,13-dihydroxy-9(*Z*)-octadecenoic acid (III) and 9,10-dihydroxy-12(*Z*)-octadecenoic acid (IV), respectively, by NbEH2.1 and StEH (Fig. 2C–E). However, no diol products were detected in the reaction containing NbEH1.1 (Fig. 2B).

It has been reported that 12(*R*),13(*S*)-epoxy-9(*S*)-hydroxy-10(*E*)-octadecenoic acid was formed by incubation of 9(*S*)-HPOD with PXG from broad bean (Hamberg and Hamberg, 1990, 1996). In our study, we also observed only one compound when 9(*S*)-HPOD was incubated with SIPXG. The major product was tentatively identified as 12(*R*),13(*S*)-epoxy-9(*S*)-hydroxy-10(*E*)-octadecenoic acid (V, Fig. 3). The Me₃Si derivative of compound V showed a mass spectrum with prominent ions at *m/z* 383 (M-15, loss of CH₃), 241 [M-157, loss of (CH₂)₇-COOCH₃], and 99 [⁺O≡C-(CH₂)₄-CH₃], which were identical with those of the Me₃Si deriva-

tive of 12(*R*),13(*S*)-epoxy-9(*S*)-hydroxy-10(*E*)-octadecenoic acid (Hamberg and Hamberg, 1996). The methyl esters of 9(*S*),12(*S*),13(*S*)-trihydroxy-10(*E*)-octadecenoic acid (Fig. 3A, first trace) and the PXG product 12(*R*),13(*S*)-epoxy-9(*S*)-hydroxy-10(*E*)-octadecenoic acid which was acid-hydrolysed (Fig. 3A, second trace) as described previously (Hamberg, 1991a; Hamberg and Hamberg, 1996) were used as references. According to previous studies (Hamberg, 1991a,b; Hamberg and Hamberg, 1996), products VI and VII (Fig. 3A) were identified as 9(*S*),12(*R*),13(*R*)- and 9(*S*),12(*S*),13(*S*)-trihydroxy-10(*E*)-octadecenoic acid (Fig. 3B). The result indicated that 12(*R*),13(*S*)-epoxy-9(*S*)-hydroxy-10(*E*)-octadecenoic acid was converted into two isomers of trihydroxyoctadecenoic acid, namely 9(*S*),12(*S*),13(*S*)- and 9(*S*),12(*R*),13(*R*)-trihydroxy-10(*E*)-octadecenoic acid, by NbEH2.1 and StEH (Fig. 3A and B). The result also revealed that StEH was much more active towards 12(*R*),13(*S*)-epoxy-9(*S*)-hydroxy-10(*E*)-octadecenoic acid than NbEH2.1. The ratio of 9(*S*),12(*S*),13(*S*): 9(*S*),12(*R*),13(*R*) isomers produced by NbEH2.1 was 58: 42, but was 36: 64 when produced by StEH. A small amount of trihydroxyoctadecenoic acid was also detected in the reactions containing only PXG protein or PXG in combination with NbEH1.1 protein. These trihydroxyoctadecenoic acids are probably derived directly from chemical hydrolysis of compound V. Recently, we demonstrated by incubation of 12,13-epoxy-9(*S*)-hydroxy-10(*E*)-octadecenoic acid in the presence of labeled H_2O^{18} with StEH (Huang and Schwab, 2012) that O^{18} is transferred to C12 and C13 of the fatty acid (ratio 1:~2.5). This observation clearly confirms the formation of two trihydroxy stereoisomers by StEH.

2.4. Inhibition of SIPXG catalytic activity by EH enzyme

We observed a phenomenon that SIPXG enzyme activity was inhibited by all three EH enzymes. Neither epoxide nor diol products were produced when SIPXG and any of the purified EHs were simultaneously incubated with fatty acids. This phenomenon was also observed in the mixture of SIPXG- and StEH-infiltrated tobacco extracts (Huang and Schwab, 2012). The inhibition could be overcome when fatty acids were incubated with SIPXG yeast extracts at first for at least 30 min, then, EH proteins were added to the reaction. As no fatty acid diol was formed by NbEH1.1, product feed-

back inhibition was excluded and protein - protein interaction between PXG and EH is assumed. To challenge this hypothesis, various amounts of purified NbEH1.1 as well as boiled NbEH1.1 (at 99 °C for 15 min, the enzyme was completely inactivated) were co-incubated with SIPXG and linoleic acid. The more NbEH1.1 was added, the less epoxide was formed (Fig. 4). Unexpected, boiled NbEH1.1 protein also inhibited the activity of SIPXG (Fig. 4). It indicated that the inhibition of the PXG enzyme activity did not depend on the activity of EH protein. The primary EH protein structure is enough to inhibit the PXG enzyme activity. However, the inhibition may not happen in a plant cell, as PXG is an integral membrane protein (Blée, 1998) and EH is a soluble protein in plants (Kiyosue et al., 1994; Stapleton et al., 1994; Arahira et al., 2000; Morisseau et al., 2000; Bellevis et al., 2002).

2.5. Expression profiles of NbEH1.1 and NbEH2.1

2.5.1. Expression of NbEH1.1 and NbEH2.1 in *N. benthamiana* treated with TMV based viral vectors and wounding

To examine whether NbEH1.1 and NbEH2.1 expression levels correlate with biotic and abiotic stress, total RNA was isolated from infiltrated leaves of *N. benthamiana* at various times after infection with tobacco mosaic virus (TMV)-based viral vectors. NbEH1.1 transcript levels increased 4 days post infiltration and continued to increase throughout the time course (Fig. 5A). In contrast, no significant induction of NbEH2.1 expression was observed in the infiltrated plants. EH enzyme activity was analyzed in the leaves treated with the viral vectors using phenyl glycidyl ether as a substrate. The activity in infiltrated leaves (10 days post infiltration) was 7-fold higher than that in untreated leaves. The effect of wounding on NbEH1.1 and NbEH2.1 gene expression was also tested by infiltration with buffer (detailed description see Experimental procedures). As a result, the level of NbEH1.1 transcripts increased strongly up to 24 h after wounding and decreased afterwards. However, wounding had no significant effect on NbEH2.1 transcript levels (Fig. 5B). Changes in EH expression levels during longer periods after buffer infiltration were not observed.

The importance of epoxide hydrolase during pathogen attack may be related to its roles in detoxification, signaling, or

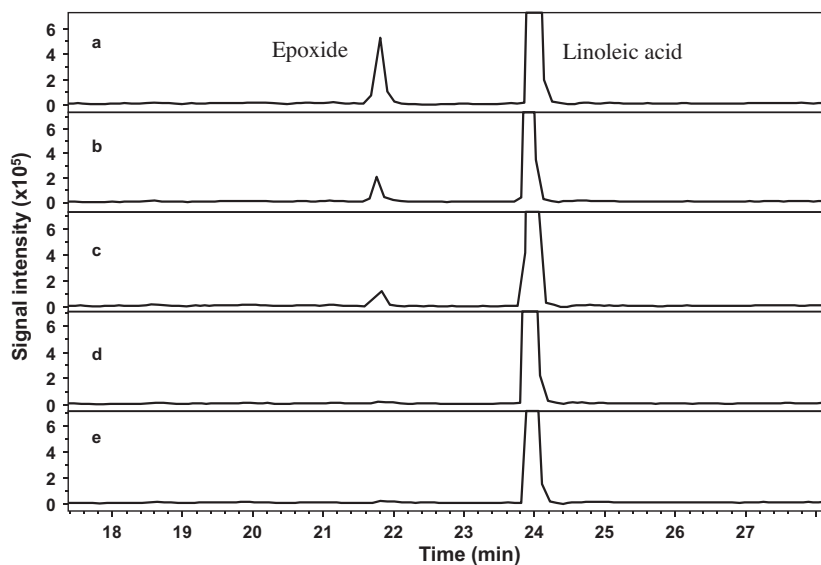


Fig. 4. Inhibition of PXG catalytic activity by NbEH1.1 protein. (a) SIPXG was incubated with linoleic acid. (b) NbEH1.1 (1 μ g) was simultaneously incubated with (a). (c) NbEH1.1 (2.5 μ g) was simultaneously incubated with (a). (d) NbEH1.1 (7.5 μ g, boiled at 99 °C for 15 min) was simultaneously incubated with (a). (e) NbEH1.1 (7.5 μ g) was simultaneously incubated with (a).

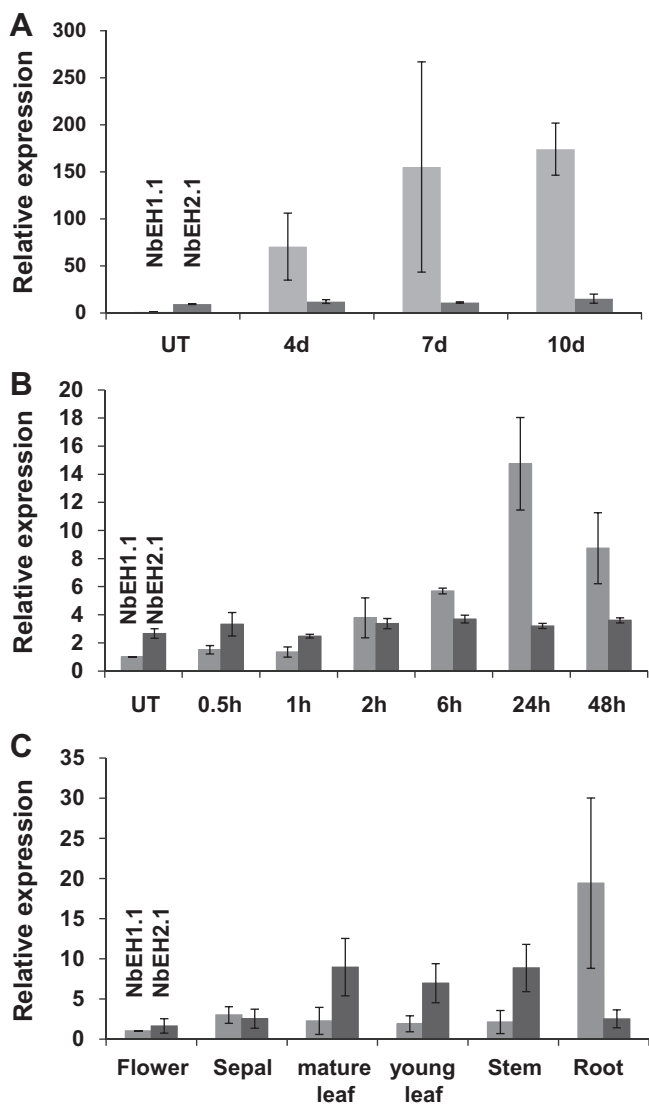


Fig. 5. Quantitative real-time RT-PCR analysis. (A) The effect of tobacco mosaic virus (TMV) on gene expression levels of *NbEH1.1* and *NbEH2.1* in *N. benthamiana*. Leaves were infiltrated with TMV based viral vectors and harvested at 4, 7, and 10 days after infiltration (4d, 7d and 10d). UT: untreated tobacco leaves. The expression level of *NbEH1.1* in untreated tobacco leaves was defined as 1. (B) The effect of wounding on gene expressions of *NbEH1.1* and *NbEH2.1* in *N. benthamiana*. Leaves were infiltrated with buffer and were harvested at 30 min, 1 h, 2 h, 6 h, 24 h, and 48 h after wounding treatment. UT: untreated tobacco leaves. The expression level of *NbEH1.1* in untreated tobacco leaves was defined as 1. (C) Spatial distribution of *NbEH1.1* and *NbEH2.1* gene transcripts in *N. benthamiana* plant. The expression level of *NbEH1.1* in flowers was defined as 1. Quantitative real-time RT-PCR analysis was performed using *NbEH1.1*, *NbEH2.1* and 18S-26S interspacer gene specific primers, the latter used as internal control for normalization. Values are means \pm SEM of three different evaluations carried out with two sets of cDNAs.

metabolism of antimicrobial compounds. Previous studies showed that *NtEH1* from *Nicotiana tabacum* was induced during the hypersensitive response to TMV (Guo et al., 1998) and *NbEH1.1*, *NbEH1.2*, *NbEH2.1* and *NbEH2.2* respond differently to various pathogens (Wijekoon et al., 2008, 2011). The results implied specialization among EH genes in basal resistance. In this study, we also demonstrated differential gene expression of *NbEH1* and *NbEH2* due to wounding and pathogen infiltration. Similarly, the transcripts of *StEH* accumulated upon wounding and application of exogenous methyl jasmonate (Stapleton et al., 1994). Other plant hormones such as auxin and ethylene have been reported to induce the expression of *AtEH* and *GmEH*, respectively (Kiyosue et al., 1994; Arahira et al., 2000).

2.5.2. Spatial distribution of *NbEH1.1* and *NbEH2.1* gene transcripts in the *N. benthamiana* plant

EHs have been localized in many cell types including seedlings, germinated seeds, roots, fruit, tubers and leaves. The expression patterns of *NbEH1.1* and *NbEH2.1* were also examined in various *N. benthamiana* organs by real-time PCR (Fig. 5C). The gene transcripts of *NbEH1.1* were present in much higher levels in roots than in flowers, sepals, leaves, and stems. The expression level in roots was 19-fold higher than the lowest level found in flowers. As the root system represents the first line of respond to pathogen attack and water stress in plants, it is not surprising that *NbEH1.1* was only expressed in roots of unstressed plants, and was induced after treatment of pathogen and wounding. Likewise, the transcript of rough lemon *RlemEH* was not detected in flowers, fruits, stems, or leaves, but was induced after inoculation of pathogen, wounding, or treatment of methyl jasmonate (Gomi et al., 2003). *NbEH2.1* gene transcripts were present predominantly in leaves and stems, with a slightly higher level in young leaves. Also, the lowest level of *NbEH2.1* gene transcripts was found in flowers. A EH gene from *Arabidopsis* (*AtEH*) whose amino acid sequence is 59% identical to *NbEH2.1* was also detected in the stems and leaves, but not in roots and flowers (Kiyosue et al., 1994). The expression level of the potato *StEH* was also found to be higher in meristematic tissue than in mature leaves (Stapleton et al., 1994).

3. Conclusion

In order to verify similarities and differences in the roles between EH1 and EH2 groups in plants, we have analysed the catalytic functions and gene expression patterns of *NbEH1.1* and *NbEH2.1* from *N. benthamiana*. The enzymes differed in substrate specificity and in contrast to *NbEH1.1*, *NbEH2.1* displayed a broad substrate range. These differences may be due to differences in the lid region around the catalytic site of the EHs (Wijekoon et al., 2011). Moreover, we showed that *NbEH2.1*, in contrast to *NbEH1.1* was active towards all fatty acid epoxides examined, similar to *StEH*. This result coincided with the sequence analysis which revealed that EH2 enzymes have a predicted peroxisome targeting signal type 1 (PTS1) C-terminus (Neuberger et al., 2003). The main functions of peroxisomes are defence against oxidative stress and β -oxidation of fatty acids (Nyathi and Baker, 2006). It is suggested that the EH2 group may be associated with peroxisomes and that they are involved in cutin monomer production in plants (Blée and Schuber, 1993).

The peroxygenase pathway has been perceived to be involved in the biosynthesis of oxylipins in response to environmental stress or in the biosynthesis of cutin polymers that are major constituents of plant surfaces (Blée, 1998). In this study, we reconstituted the peroxygenase pathway *in vitro* using a mixture of SIPXG yeast extract and purified recombinant EH proteins. Only the incubation of the mixture of SIPXG and EH2 proteins with oleic acid, *cis*-11-eicosenoic acid, linoleic acid, and 9(S)-HPOD produced a high level of diols or triols. This supported the suggestion that EH2 but not EH1 are involved in cutin monomer production in plants. Our data also showed differential gene expression levels of *NbEH1.1* and *NbEH2.1* in response to pathogen and wounding as well as in various organs in *N. benthamiana*. Thus, they are differently regulated and may serve diverse roles.

Overall, different isoforms of EHs probably exhibit different biochemical and biological functions in plants as they accept different epoxide substrates and show various expression patterns. Our results showed that *NbEH1.1* only accepted aromatic epoxides such as phenyl glycidyl ether and styrene oxide as substrates. As *NbEH1.1* was induced by TMV and wounding (this study) and had increased expression during compatible interactions with

some pathogens (Wijekoon et al., 2008), it may play a role in generating signals for activation of certain defence responses in tobacco. However, EH2 enzymes which contain a predicted peroxisomal targeting sequence at the C terminus, hydrate efficiently fatty acid epoxides to form diols and are uniformly expressed in different tissues may be associated with peroxisomes and are probably involved in cutin monomer production in plants.

4. Experimental

4.1. Chemicals

Commercial chemicals were purchased in analytical grade from the following companies: linoleic acid (Roth, Karlsruhe, Germany); oleic acid, *cis*-11-eicosenoic acid, *cis*-stilbene oxide, *trans*-stilbene oxide, *trans*-1,3-diphenyl-2,3-epoxypropan-1-one, phenyl glycidyl ether, styrene oxide, 1,2-epoxypentane, and glycidyl isopropyl ether (Sigma-Aldrich, Steinheim, Germany); rac *cis*-9,10-epoxystearic acid (Biozol Diagnostica, Eching, Germany). 9(*S*)-HPOD was synthesized from linoleic acid using Nb-9-LOX from *N. benthamiana* (Huang and Schwab, 2011).

4.2. Treatment of plant materials

N. benthamiana was grown in a growth room maintained at 23 ± 1 °C with a 16 h light/8 h dark photoperiod and a light intensity of 70 ± 10 $\mu\text{mol m}^{-2} \text{s}^{-1}$. Leaves used for treatment of wounding or infiltration of the viral vectors were taken from plants about 7–10 weeks old. For investigation of the effects of wounding on *NbEH1.1* and *NbEH2.1* gene expression, leaves of *N. benthamiana* were infiltrated with buffer (10 mM 2-*N*-morpholino-ethanesulfonic acid (MES) pH 5.5, 10 mM MgSO_4) and were harvested at 30 min, 1 h, 2 h, 6 h, 24 h, and 48 h after wounding. The description of the viral vectors and agroinfiltration of tobacco leaves were previously reported (Huang and Schwab, 2011). The tobacco leaves harvested 4, 7, and 10 days after infiltration were used for real time PCR analysis.

4.3. Real-time RT-PCR analysis

Total RNA was extracted from *N. benthamiana* using the CTAB extraction procedure (Liao et al., 2004). RNA samples were treated with RNase free DNase I (Fermentas, St. Leon-Roth, Germany) for 1 h at 37 °C. First strand cDNA synthesis was performed in duplicate in a 20 μl reaction volume, with 1 μg of total RNA as the template, random primer (random hexamer, 100 pmol), and M-MLV reverse transcriptase (200 U, Invitrogen, Karlsruhe, Germany) according to the manufacturer's instructions. Real-time PCR was performed as described by Huang et al. (2010). Relative quantification of gene expression was performed using an 18S–26S interspacer gene as a reference (Pfaffl, 2001). Primers used are listed in Supplementary Table S1.

4.4. Heterologous expression and purification of *NbEH1.1*, *NbEH2.1* and *StEH*

Total RNA was isolated from leaves of *N. benthamiana* treated with viral vectors and potato tuber (*Solanum tuberosum*) by CTAB extraction (Liao et al., 2004). The first-strand cDNAs were synthesized from 10 μg of total RNA using Superscript III RTase (Invitrogen, Karlsruhe, Germany) and a GeneRacer oligo-dT primer (5'-GCT GTC AAC GAT ACG CTA CGT AAC GGC ATG ACA GTG T₍₁₈₎-3').

The coding regions of *NbEH1.1*, *NbEH2.1*, and *StEH* were amplified by RT-PCR with the corresponding cDNA template and primers designed on the basis of a tobacco *NtEH* gene (Genbank accession

number U57350), a tobacco *NbEH2* gene (Genbank accession number EU779658), and a potato *EH* gene (Genbank accession number U02497), respectively. The PCR primers used for each gene are listed in Supplementary Table S2. The temperature program used was 5 min at 95 °C, 1 cycle; 45 s at 95 °C, 45 s at 55 °C, 2 min at 72 °C, 35 cycles; final extension at 72 °C for 10 min. The PCR products were double digested with restriction enzymes, the recognition sequences (underlined) of which are contained in the primers (Supplementary Table S2), and then ligated with the pQE30 vector (QIAGEN, Hilden, Germany) to yield pQE30-*NbEH1.1*, pQE30-*NbEH2.1* and pQE30-*StEH*. The recombinant genes were subjected to sequencing to confirm the sequence of the inserts. Furthermore, these three constructs and empty vector (negative control) were transformed into the M15 (pREP4) cell strain for expression of recombinant protein. A 4 ml overnight culture was used to inoculate a 400 ml culture in LB medium containing 100 $\mu\text{g ml}^{-1}$ ampicillin and 25 $\mu\text{g ml}^{-1}$ kanamycin. Cultures were grown at 37 °C until an OD₆₀₀ of 0.6 was reached. Expression of the protein was induced by the addition of 0.2 mM IPTG, and the cultures were grown at 18 °C for an additional 20 h. Cells were harvested by centrifugation (5000g, 20 min, 4 °C) and resuspended in 10 ml binding buffer (20 mM sodium phosphate buffer, 500 mM NaCl, 20 mM imidazole, pH 7.4). Cells were lysed by sonication on ice with a MS 73 sonotrode (Bandelin electronic, Berlin Germany) 10 times for 30 s at 10% of maximal power. Cell debris was removed by centrifugation (12,000g, 30 min, 4 °C). Purification of the expression products of *NbEH1.1*, *NbEH2.1* and *StEH* were performed using a His trap affinity column (GE Healthcare, Freiburg, Germany), prepacked with precharged Ni Sepharose 6 fast flow, according to manufacturer's instructions. Proteins were analyzed by SDS-PAGE with 10% polyacrylamide gels and stained with Coomassie brilliant blue R-250. The protein concentration was determined by the Bradford assay (Bradford, 1976).

4.5. Enzyme assays

EH activities towards various substrates were determined by LC-MS and GC-MS as described below.

For aromatic epoxide substrates (Supplementary Fig. S1A), EH activity was determined by LC-MS. Purified proteins were incubated with 300 μM substrate in 500 μl of 1 \times PBS buffer (140 mM NaCl, 8 mM Na_2HPO_4 , 2.7 mM KCl, 1.76 mM KH_2PO_4 , pH 7.4) for 30 min at 30 °C. The reaction products were extracted with the same volume of ethyl acetate, evaporated to dryness, resuspended in methanol, and analysed by LC-MS (method I, see below).

For terminal aliphatic epoxide (Supplementary Fig. S1B) and limonene epoxide (Supplementary Fig. S1C) substrates, EH activity was determined by SPME-GC-MS. Purified proteins were diluted to 2 ml of 1 \times PBS buffer containing 300 μM substrate. The mixture was incubated for 30 min at 30 °C with constant shaking in a 20 ml reaction vial closed with a septum. Headspace compounds were trapped by SPME (65 μm polydimethylsiloxane-divinylbenzene coated fibre, Supelco, Steinheim, Germany) at 45 °C for 30 min and analysed by GC-MS (method I for terminal aliphatic epoxide substrates and method II for limonene epoxide substrates, see below).

Fatty acid epoxides (Supplementary Fig. S1D, except for *cis*-9,10-epoxystearic acid) were prepared by incubation of corresponding fatty acids with SIPXG (peroxygenase from tomato) yeast extract (Aghofack-Nguemezi et al., 2011) at 30 °C in buffer C (10 mM sodium acetate buffer, pH 6.0, 2% glycerol, 0.01% Tween 20) containing 2.5 mM hydrogen peroxide and 300 μM of fatty acid with constant shaking for 60 min. The PXG products were partitioned into ethyl acetate, evaporated to dryness, and further used as substrates for EH enzyme assays. Purified EH proteins were incubated with various fatty acid epoxides in excess in 500 μl of

1 × PBS buffer for 30 min at 30 °C. The reaction products were extracted with the same volume of ethyl acetate, evaporated to dryness, re-suspended in methanol, and analysed by LC–MS (method II, see below). Products formed from 9(*S*)-HPOD with SIPXG in combination with each EH were isolated by extraction with ethyl acetate, methylated and trimethylsilylated, and then subjected to GC–MS (Aghofack-Nguemezi et al., 2011).

Amounts of aromatic diol products were determined using a standard curve calculated from various known concentrations of corresponding substrates against the UV peak areas which were recorded at 254 nm. Amounts of fatty acid diol products were determined using a standard curve calculated from various known concentrations of *cis*-9,10-epoxystearic acid (Biozol, Diagnostica, Eching, Germany) against the mass peak areas which were recorded by LC–MS. Amounts of trihydroxyoctadecenoic acid products were determined using a standard curve calculated from various known concentrations of methylated and trimethylsilylated 9(*S*),12(*S*),13(*S*)-trihydroxy-10(*E*)-octadecenoic acid against the mass peak areas which were recorded by GC–MS.

The pH optimum of NbeH1.1 and NbeH2.1 was determined using different buffers for various pH ranges: 50 mM citric acid (pH 2.0–6.0), 50 mM sodium phosphate (pH 6.0–8.0), and 50 mM Tris–HCl (pH 8.0–12.0) in 0.5-U intervals. The optimal temperature was evaluated from 15 to 60 °C in 5 °C intervals at pH 7.4 (Supplementary Fig. S2). The kinetic parameters were determined under optimum conditions and were calculated by triplicate determinations using Microsoft Excel Solver (Supplementary Fig. S3).

4.6. High performance liquid chromatography–electrospray ionization mass spectrometry (LC–MS)

The HPLC system consisted of a quaternary pump and a variable wavelength detector, all from Agilent 1100 (Bruker Daltonics, Bremen, Germany). The column was a LUNA C18 100A 150 × 2 mm (Phenomenex, Aschaffenburg, Germany). HPLC was performed with the following binary gradient system: solvent A, water with 0.1% formic acid and solvent B, 100% methanol with 0.1% formic acid. Two different gradient programs were used: Method I: 0–10 min, 50% A/50% B to 100% B, hold for 5 min; 15–20 min, 100% B to 50% A/50% B, hold for 10 min; method II: 0–10 min, 70% A/30% B to 50% A/50% B; 10–40 min, 50% A/50% B to 100% B, hold for 5 min; 100% B to 70% A/30% B, in 1 min, then hold for 6 min. The flow rate was 0.2 ml min⁻¹. Attached to the HPLC was a Bruker esquire 3000plus mass spectrometer with an ESI interface that was used to record the mass spectra. The ionization voltage of the capillary was 4000 V and the end plate was set to –500 V. Products were monitored using diagnostic ions listed in Supplementary Table S3.

4.7. Gas chromatography–mass spectrometry (GC–MS)

The volatile compounds collected from the headspace were analysed on a Thermo Finnigan Trace DSQ mass spectrometer coupled to a 0.25 μm BPX5 20 M fused silica capillary column with a 30 m × 0.25 mm inner diameter. He (1.1 ml min⁻¹) was used as carrier gas. The injector temperature was 250 °C, set for splitless injection. The temperature program for method I was 40 °C for 8 min, 40–100 °C at a rate of 4 °C min⁻¹, and 100–190 °C at a rate of 30 °C min⁻¹, then hold for 5 min, whereas for method II: 40 °C for 5 min, 40–100 °C at a rate of 8 °C min⁻¹, and 100–280 °C at a rate of 40 °C min⁻¹. The ion source temperature was 250 °C. Mass range was recorded from *m/z* 50 to 300 and spectra were evaluated with the Xcalibur software version 1.4 supplied with the device. Diagnostic ions for detection of products were listed in Supplementary Table S3.

Acknowledgements

Financial Support by the German Federal Ministry of Nutrition, Agriculture and Consumer Protection (BMELV) and FNR (SynRg) is gratefully acknowledged. The reference compound 9(*S*),12(*S*),13(*S*)-trihydroxy-10(*E*)-octadecenoic acid was kindly provided by Mats Hamberg.

Appendix A. Supplementary data

Supplementary data associated with this article can be found, in the online version, at <http://dx.doi.org/10.1016/j.phytochem.2013.02.020>.

References

- Aghofack-Nguemezi, J., Fuchs, C., Yeh, S.-Y., Huang, F.-C., Hoffmann, T., Schwab, W., 2011. An oxygenase inhibitor study in *Solanum lycopersicum* combined with metabolite profiling analysis revealed a potent peroxygenase inactivator. *J. Exp. Bot.* 62, 1313–1323.
- Arahira, M., Nong, V.H., Udaka, K., Fukazawa, C., 2000. Purification, molecular cloning and ethylene-inducible expression of a soluble-type epoxide hydrolase from soybean (*Glycine max* [L.] Merr.). *Eur. J. Biochem.* 267, 2649–2657.
- Bellevik, S., Zhang, J., Meijer, J., 2002. *Brassica napus* soluble epoxide hydrolase (BNSEH1). *Eur. J. Biochem.* 269, 5295–5302.
- Blée, E., 1998. Biosynthesis of phytooxylipins: the peroxygenase pathway. *Fett/Lipid* 100, 121–127.
- Blée, E., Schuber, F., 1990. Efficient epoxidation of unsaturated fatty acids by hydroperoxide-dependent oxygenase. *J. Biol. Chem.* 265, 12887–12894.
- Blée, E., Schuber, F., 1992a. Enantioselectivity of the hydrolysis of linoleic acid monoepoxides catalyzed by soybean fatty acid epoxide hydrolase. *Biochem. Biophys. Res. Commun.* 187, 171–177.
- Blée, E., Schuber, F., 1992b. Regio- and enantioselectivity of soybean fatty acid epoxide hydrolase. *J. Biol. Chem.* 267, 11881–11887.
- Blée, E., Schuber, F., 1993. Biosynthesis of cutin monomers: involvement of a lipoxigenase/peroxygenase pathway. *Plant J.* 4, 113–123.
- Blée, E., Schuber, F., 1995. Sterecontrolled hydrolysis of the linoleic acid monoepoxide regioisomers catalyzed by soybean epoxide hydrolase. *Eur. J. Biochem.* 230, 229–234.
- Blée, E., Summerer, S., Flenet, M., Rogniaux, H., Dorsselaer, A.V., Schuber, F., 2005. Soybean epoxide hydrolase: identification of the catalytic residues and probing of the reaction mechanism with secondary kinetic isotope effects. *J. Biol. Chem.* 280, 6479–6487.
- Bradford, M.M., 1976. A rapid and sensitive for the quantitation of microgram quantities of protein utilizing the principle of protein–dye binding. *Analytical Biochem.* 72, 248–254.
- Edqvist, J., Farbos, I., 2003. A germination-specific epoxide hydrolase from *Euphorbia lagascae*. *Planta* 216, 403–412.
- Elfström, L.T., Widersten, M., 2005. Catalysis of potato epoxide hydrolase, StEH1. *Biochem. J.* 390, 633–640.
- Gomi, K., Yamamoto, H., Akimitsu, K., 2003. Epoxide hydrolase: a mRNA induced by the fungal pathogen *Alternaria alternata* on rough lemon (*Citrus jambhiri* Lush). *Plant Mol. Biol.* 53, 189–199.
- Guo, A., Durner, J., Klessig, D.F., 1998. Characterization of a tobacco epoxide hydrolase gene induced during the resistance response to TMV. *Plant J.* 15, 647–656.
- Hamberg, M., Hamberg, G., 1990. Hydroperoxide-dependent epoxidation of unsaturated fatty acids in the broad bean (*Vicia faba* L.). *Arch. Biochem. Biophys.* 283, 409–416.
- Hamberg, M., 1991a. Regio- and stereochemical analysis of trihydroxyoctadecenoic acids derived from linoleic acid 9- and 13-hydroperoxides. *Lipids* 26, 407–415.
- Hamberg, M., 1991b. Trihydroxyoctadecenoic acids in beer: qualitative and quantitative analysis. *J. Agric. Food Chem.* 39, 1568–1572.
- Hamberg, M., Fahlstadius, P., 1992. On the specificity of a fatty acid epoxygenase in broad bean (*Vicia faba* L.). *Plant Physiol.* 99, 987–995.
- Hamberg, M., Hamberg, G., 1996. Peroxygenase-catalyzed fatty acid epoxidation in cereal seeds. *Plant Physiol.* 110, 807–815.
- Huang, F.-C., Schwab, W., 2011. Cloning and characterization of a 9-lipoxygenase gene induced by pathogen attack from *Nicotiana benthamiana* for biotechnological application. *BMC Biotechnol.* 11, 30.
- Huang, F.-C., Studart-Witkowski, C., Schwab, W., 2010. Overexpression of hydroperoxide lyase gene in *Nicotiana benthamiana* using a viral vector system. *Plant Biotech.* J. 8, 1–13.
- Huang, F.-C., Schwab, W., 2012. Overexpression of hydroperoxide lyase, peroxygenase and epoxide hydrolase in tobacco for the biotechnological production of flavours and polymer precursors. *Plant Biotech. J.* 10, 1099–1109.
- Kato, T., Yamaguchi, Y., Uyehara, T., Yokoyama, T., Namai, T., Yamanaka, S., 1983. Defense mechanism of the rice plant against rice blast disease. *Naturwissenschaften* 70, 200–201.
- Kiyosue, T., Beetham, J.K., Pinot, F., Hammock, B.D., Yamaguchi-Shinozaki, K., Shinozaki, K., 1994. Characterization of an Arabidopsis cDNA for a soluble

- epoxide hydrolase gene that is inducible by auxin and water stress. *Plant J.* 6, 259–269.
- Liao, Z., Chen, M., Guo, L., Gong, Y., Tang, F., Sun, X., Tang, K., 2004. Rapid isolation of high-quality total RNA from *Taxus* and *Ginkgo*. *Prep. Biochem. Biotech.* 34, 209–214.
- Morisseau, C., Beetham, J.K., Pinot, F., Debernard, S., Newman, J.W., Hammock, B.D., 2000. Cress and potato soluble epoxide hydrolases: purification, biochemical characterization, and comparison to mammalian enzymes. *Arch. Biochem. Biophys.* 378, 321–332.
- Morisseau, C., Hammock, B.D., 2005. Epoxide hydrolases: mechanisms, inhibitor designs, and biological roles. *Ann. Rev. Pharmacol. Toxicol.* 45, 31–333.
- Mowbray, S.L., Elfström, L.T., Ahlgren, K.M., Andersson, C.E., Widersten, M., 2006. X-ray structure of potato epoxide hydrolase sheds light on substrate specificity in plant enzymes. *Protein Sci.* 15, 1628–1637.
- Murray, G.I., Peterson, P.J., Weaver, R.J., Ewen, S.W., Melvin, W.T., Burke, M.D., 1993. The expression of cytochrome P-450, epoxide hydrolases, and glutathione S-transferase in hepatocellular carcinoma. *Cancer* 71, 36–43.
- Neuberger, G., Maurer-Stroh, S., Eisenhaber, B., Hartig, A., Eisenhaber, F., 2003. Prediction of peroxisomal targeting signal 1 containing proteins from amino acid sequence. *J. Mol. Biol.* 328, 581–592.
- Newman, J.W., Morisseau, C., Hammock, B.D., 2005. Epoxide hydrolases: their roles and interactions with lipid metabolism. *Prog. Lipid Res.* 44, 1–51.
- Nyathi, Y., Baker, A., 2006. Plant peroxisomes as a source of signaling. *Biochim. Biophys. Acta* 1763, 1478–1495.
- Pfaffl, M.W., 2001. A new mathematical model for relative quantification in real-time RT-PCR. *Nucleic Acids Res.* 29, 2002–2007.
- Pinot, F., Skrabs, M., Compagnon, V., Salaün, J.P., Benveniste, I., Schreiber, L., Durst, F., 2000. Omega-hydroxylation of epoxy- and hydroxyl- fatty acids by CYP94A1: possible involvement in plant defense. *Biochem. Soc. Trans.* 28, 867–870.
- Stapleton, A., Beetham, J.K., Pinot, F., Garbarino, J.E., Rockhold, D.R., Friedman, M., Hammock, B.D., Belknap, W.R., 1994. Cloning and expression of soluble epoxide hydrolase from potato. *Plant J.* 6, 251–258.
- Thomaeus, A., Naworyta, A., Mowbray, S.L., Widersten, M., 2008. Removal of distal protein–water hydrogen bonds in a plant epoxide hydrolase increases catalytic turnover but decreases thermostability. *Protein Sci.* 17, 1275–1284.
- Van der Werf, M.J., Swarts, H.J., Bont, J.A., 1999. *Rhodococcus erythropolis* DCL14 contains a novel degradation pathway for limonene. *Appl. Environ. Microbiol.* 65, 2095–2102.
- Wijekoon, C.P., Goodwin, P.H., Hsiang, T., 2008. The involvement of two epoxide hydrolase genes, *NbEH1.1* and *NbEH1.2* of *Nicotiana benthamiana* in the interaction with *Colletotrichum destructivum*, *Colletotrichum orbiculare* or *Pseudomonas syringae* pv. *tabaci*. *Functional Plant Biol.* 35, 1112–1122.
- Wijekoon, C.P., Goodwin, P.H., Valliani, M., Hsiang, T., 2011. The role of a putative peroxisomal-targeted epoxide hydrolase of *Nicotiana benthamiana* in interactions with *Colletotrichum destructivum*, *C. orbiculare* or *Pseudomonas syringae* pv. *tabaci*. *Plant Sci.* 181, 177–187.